Available online at www.sciencedirect.com
ScienceDirect
Journal of Nuclear Materials 374 (2008) 334–337
journal of nuclear materials
www.elsevier.com/locate/jnucmat

Letter to the Editors

Small-angle neutron scattering study of neutron-irradiated iron and an iron–nickel alloy

F. Bergner [a,*], A. Ulbricht [a], M. Hernandez-Mayoral [b], P.K. Pranzas [c]

[a] Forschungszentrum Dresden-Rossendorf, Institute of Safety Research, P.O. Box 510119, 01314 Dresden, Germany
[b] CIEMAT, Avenida Complutense 22, 28040 Madrid, Spain
[c] GKSS Forschungszentrum, Max-Planck-Strasse, 21502 Geesthacht, Germany

Received 19 April 2007; accepted 12 July 2007

Abstract

The nature of irradiation-induced features in Fe–3wt%Ni was investigated by means of small-angle neutron scattering and hardness measurements and compared with results for commercially pure Fe. We have observed a three times larger volume fraction of irradiation-induced scatterers for the Fe–Ni alloy than for pure Fe. A vacancy–Ni ratio of 0.4–0.5 was deduced for the average scatterer. This finding is consistent with the hardness increase observed.

1. Introduction

Ni is an important alloying element of both reactor pressure vessel (RPV) steels and austenitic stainless steels used for RPV internals. It plays a key role in the degradation mechanism of neutron-irradiated RPV steels. A synergistic effect of the elements Cu and Ni on the irradiation-induced degradation of mechanical properties was identified [1]. Irradiation-induced defect-solute clusters were found to be enriched with Ni relative to the matrix level in both low- and medium-Cu RPV steels [2]. In order to achieve a more rigorous understanding of the kinetics of formation and the nature of the irradiation-induced features and the resulting property degradation, a multiscale multiphysics modeling approach was stimulated [3]. Experimental results at the relevant nm-size scale are required for simple binary systems such as Fe–Ni for the purpose of validation of the modeling tools based on molecular dynamics, Monte-Carlo simulations and cluster dynamics. The aim of the paper is to present results for neutron-irradiated commercially pure Fe (denoted Fe below) and an Fe–3wt%Ni alloy obtained by small-angle neutron scattering (SANS) and Vickers hardness measurements. The nature of the irradiation-induced scatterers is discussed in some detail.

2. Experimental procedure and analysis

The materials investigated are commercially pure Fe (<0.01 wt%C) and Fe–3wt%Ni (Table 1). Specimens of 5 mm diameter and 1 mm thickness were taken from heads of tensile specimens irradiated at NRI Řež (Czech Republic) at an irradiation temperature of 290 °C up to a neutron fluence of $3.8\times10^{23}\,m^{-2}$ ($E>0.5$ MeV), which corresponds to about 0.038 displacements per atom (dpa). The fluence rate was about $3\times10^{17}\,m^{-2}\,s^{-1}$. The SANS measurements were carried out at the SANS-2 instrument of the GeNF facility of GKSS [4] at a wavelength of 0.58 nm with sample-detector distances of 1 and 4 m. The samples were placed in a saturation magnetic field of 1.7 T. Due to the small sample diameter a measuring time four times longer than standard was needed in order to gain comparable data statistics. The data analysis is described in [5] including corrections related to both sample holder and detector, absolute calibration as well as separa-

* Corresponding author. Tel.: +49 351 260 3186; fax: +49 351 260 2205.
E-mail address: f.bergner@fzd.de (F. Bergner).

0022-3115/$ - see front matter © 2007 Elsevier B.V. All rights reserved.
doi:10.1016/j.jnucmat.2007.07.008

Table 1
Summary of experimental results

Material	Volume fraction, c (%)	Peak radius, R_p (nm)	A-ratio	Vickers hardness, HV10	
				Unirradiated	0.038 dpa
Pure Fe	0.006 ± 0.004	0.78 ± 0.05	1.4 ± 0.2	81 ± 3	132 ± 5
Fe–3wt%Ni	0.019 ± 0.007	0.85 ± 0.05	2.4 ± 0.1	114 ± 2	155 ± 4

tion of magnetic and nuclear scattering cross-sections. The coherent scattering cross-section can be expressed as

$$\left(\frac{d\Sigma}{d\Omega}\right)_c(\vec{Q}) = \frac{N}{V_p}\Delta\eta^2 V^2(R)|F(\vec{Q},R)|^2 \quad (1)$$

for a number of N homogeneous spherical scatterers of radius, R, in the probed volume, V_p. V is the volume of a sphere of radius, R, $\vec{Q} = (Q_x, Q_y, Q_z)$ is the scattering vector, $Q = |\vec{Q}|$, and F is the form factor

$$|F(\vec{Q},R)|^2 = \frac{9(\sin QR - QR\cos QR)^2}{(QR)^6}. \quad (2)$$

Magnetic and nuclear scattering are not distinguished in Eq. (1). The scattering contrast, $\Delta\eta$, is given by

$$\Delta\eta_i^2 = \left[(n\bar{b}_i)_S - (n\bar{b}_i)_M\right]^2, \quad (3)$$

where $i = m$ for magnetic scattering and $i = n$ for nuclear scattering. Subscripts S and M refer to scatterer and matrix, respectively, and $\bar{b}_m$ and $\bar{b}_n$ denote the average scattering length for magnetic and nuclear scattering, respectively. In the case of non-magnetic scatterers ($\bar{b}_{m,S} = 0$) in pure Fe

$$\Delta\eta_m^2 = (n_{Fe}b_{m,Fe})^2. \quad (4)$$

For dislocation loops [6] the above separation of terms is impractical and the cross-section is approximately expressed as

$$\left(\frac{d\Sigma}{d\Omega}\right)_c(\vec{Q}) = \frac{N}{V_p}\Delta\eta^2\left[\left(\frac{1-2\nu}{1-\nu}\right)\frac{2\pi bR\sqrt{Q_x^2+Q_y^2}}{Q^2}J_1\left(R\sqrt{Q_x^2+Q_y^2}\right)\right]^2, \quad (5)$$

where ν is the Poisson ratio, b is the Burgers vector of the dislocation loop and J_1 is the Bessel function.

The indirect transformation method [7] based on a description of the size distribution by a number of 40 cubic spline functions in the radius range from 0 to 15 nm is applied to obtain the size distribution of scatterers by means of a weighted least-squares procedure without assuming a certain type of distribution. The unirradiated control of pure Fe is subtracted after performing the transformation not only for irradiated Fe but also for irradiated Fe–3%Ni.

3. Results and discussion

The separated magnetic and nuclear coherent scattering cross-sections are given in Fig. 1. A pronounced irradiation-induced increase is observed at scattering vectors, $Q > 0.5\ nm^{-1}$ and $Q > 0.9\ nm^{-1}$, for magnetic and nuclear scattering, respectively, for both Fe and Fe–3wt%Ni. In addition, a slight, weakly Q-dependent increase of the nuclear scattering cross-section is found for Fe. The latter effect could be attributed to a distribution of dislocation loops identified by TEM for Fe irradiated at a similar fluence ($3.5 \times 10^{23}\ m^{-2}$, $E > 1$ MeV, about 0.051 dpa) and temperature (300 °C). A typical TEM micrograph and the measured size distribution are shown in Fig. 2. The total number density estimated from the TEM analysis is $0.85 \times 10^{21}\ m^{-3}$. The nuclear scattering cross-section caused by this distribution was calculated on the basis of Eq. (5) according to [6]. The result is compared in Fig. 3 with the measured nuclear scattering cross-section for Fe. We have found that the dislocation loops are definitely not responsible for the observed difference of the nuclear scattering cross-sections for unirradiated and irradiated Fe. This difference has to be attributed to a sample-related variance in the lower Q-range and to experimental uncertainties. The analysis also indicates that the difference of

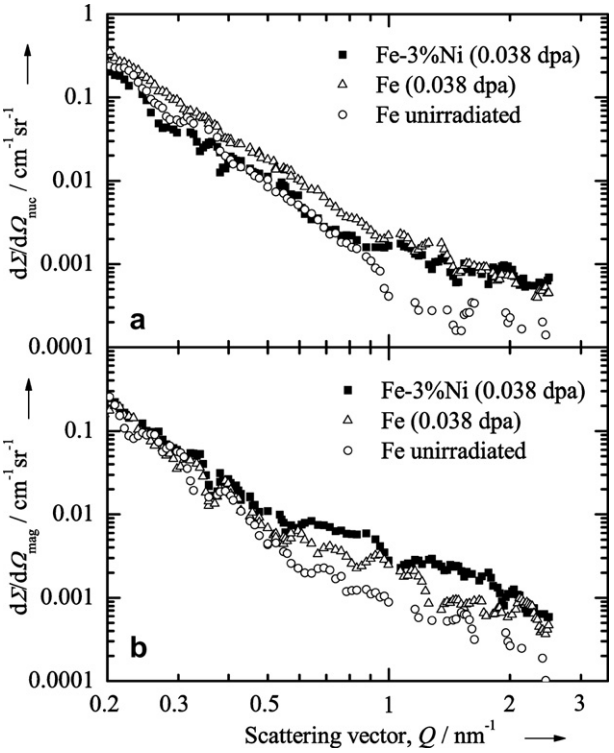

Fig. 1. Coherent nuclear (a) and magnetic (b) scattering cross-sections for Fe and Fe–3%Ni both neutron-irradiated up to 0.038 dpa and for unirradiated Fe.

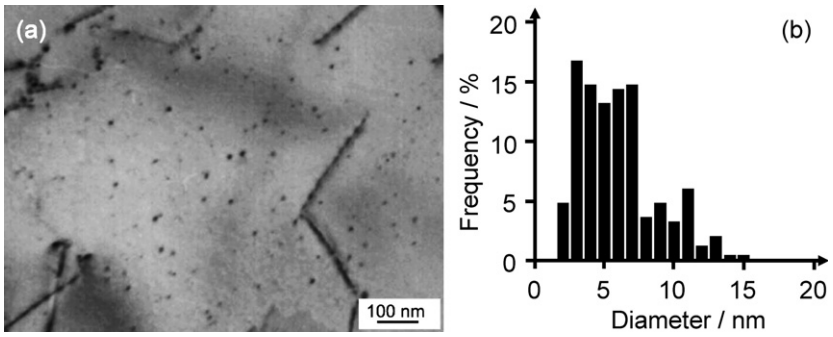

Fig. 2. TEM image (a) and size distribution (b) of dislocation loops in neutron-irradiated Fe (0.051 dpa).

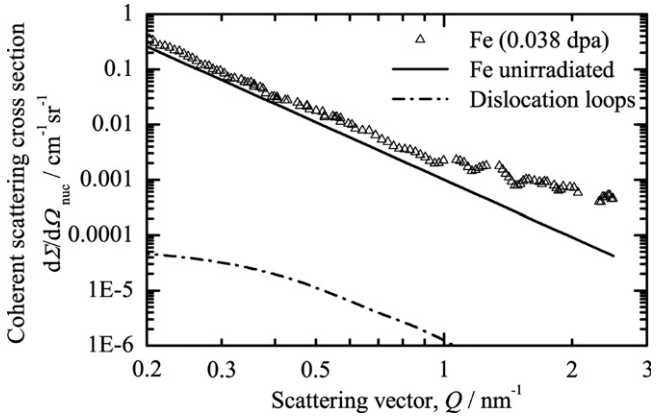

Fig. 3. Nuclear scattering cross-section calculated for the size distribution of dislocation loops (Fig. 2), scattering curve fitted to the unirradiated Fe reference from Fig. 1(a) and comparison with measured data of neutron-irradiated Fe.

the scattering curves for irradiated Fe–3wt%Ni and unirradiated Fe is not caused by dislocation loops.

The present investigation is focused on the pronounced effects at Q-values larger than 0.5 nm^{-1}. The size distribution of irradiation-induced scatterers was calculated on the assumption of homogeneous non-magnetic spherical scatterers, Eqs. (1), (2), and (4). The parameters characterizing the size distribution, peak radius and volume fraction, are summarized in Table 1. The volume fractions are lower bounds and have to be scaled up in relation to the magnetic contrast, Eq. (3), if the scatterers are characterized by a non-zero magnetic scattering length. The number density of scatterers deduced from the SANS measurement for pure Fe, 3×10^{22} m^{-3}, is 35 times higher than the number density of loops deduced from TEM. This result is not inconsistent with the TEM results (Fig. 2), because the size distribution decays at a radius of 1.3 nm, i.e. essentially below the detection limit of TEM. The A-ratio defined as the ratio of scattered intensities perpendicular and parallel to the direction of the saturation magnetic field [8] and Vickers hardness at a load of 98.1 N, HV10, are also given in Table 1.

The A-ratio was calculated according to Eq. (6) for different compositions of the scatterers in Fe–3wt%Ni including different fractions of vacancies, Ni atoms and Fe atoms confined to bcc lattice sites (coherent clusters or atmospheres)

$$A=\frac{(\mathrm{d}\Sigma/\mathrm{d}\Omega)_{\perp}}{(\mathrm{d}\Sigma/\mathrm{d}\Omega)_{\parallel}}=1+\frac{\Delta\eta_m^2}{\Delta\eta_n^2}=1+\left(\frac{6.0(n_{\mathrm{Fe}}-1)+1.0n_{\mathrm{Ni}}}{9.45(n_{\mathrm{Fe}}-1)+10.3n_{\mathrm{Ni}}}\right)^2. \tag{6}$$

$\Delta\eta_m^2$ and $\Delta\eta_n^2$ denote magnetic and nuclear contrasts [8], respectively, integrated over the relevant size range, $R<2$ nm, in the present case. In Eq. (6), the coefficients in the nominator are the values in units of fm (10^{-15} m) of the magnetic scattering length for Fe and Ni, the coefficients in the denominator are the values in units of fm of the nuclear scattering length for Fe and Ni. The fractions of Fe atoms, n_{Fe}, and Ni atoms, n_{Ni}, are confined by the condition $n_{\mathrm{Fe}}+n_{\mathrm{Ni}}=1-n_{\mathrm{v}}$. The results of the calculations are plotted in Fig. 4 as a function of the ratio of the fractions of vacancies, n_{v}, and Ni atoms, n_{Ni}, in the average scatterer. We have observed that

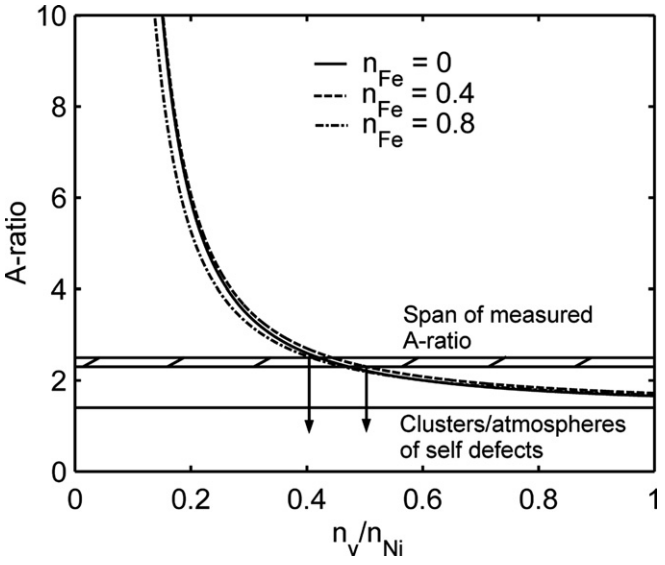

Fig. 4. Span of measured and calculated A-ratios of coherent vacancy–Ni–Fe clusters as a function of the ratio of vacancy and Ni fractions, $n_{\mathrm{v}}/n_{\mathrm{Ni}}$.

- the value of the measured A-ratio of 1.4 ± 0.2 for pure Fe (Table 1) is in agreement with the value expected for vacancy clusters or depleted zones, $A = 1.4$ (Fig. 4),
- the ratio of the vacancy fraction and the fraction of Ni atoms in the average scatterer is between 0.4 and 0.5 (see arrows) and
- the A-ratio is almost insensitive to the fraction of Fe atoms in the average scatterer.

It is important to note that the measured A-ratio of 2.4 is incompatible with non-magnetic fcc Fe–Ni particles, which would yield values of the A-ratio in excess of 10.

Considering pure Fe, SANS cannot distinguish between true vacancy clusters (i.e. scatterers containing one vacancy per lattice site) and depleted zones (i.e. scatterers containing considerably less than one vacancy per lattice site). Positron lifetime measurements confirm the presence of vacancy clusters and point to cluster sizes of 66 vacancies [9], which correspond to a radius of 0.57 nm in comparison with a peak radius of 0.75 nm deduced from the present SANS experiment. A decision in favour of vacancy clusters or depleted zones cannot be made here. In fact, both the irradiation conditions and the procedures to obtain average radii from positron lifetime or SANS are different. Furthermore, the positron lifetime is rather insensitive to cluster sizes in excess of 66 vacancies [9]. However, if we assume depleted zones, the total volume fraction of scatterers given in Table 1 has to be scaled up in inverse proportion with the contrast (see Eq. (1)), in order to fit the experimentally observed scattering cross-sections. The reduction of contrast is directly proportional to the decrease of the vacancy fraction in the depleted zones. Therefore, the total volume fraction taken by the vacancy part of the scatterers is independent of the nature of the scatterers (true vacancy cluster or depleted zone) and is well represented by the value given in Table 1. A similar reasoning also applies to the unknown Fe fraction (or vacancy + Ni fraction) in the scatterers observed for Fe–3wt%Ni.

The observed difference in the Q-values, at which the magnetic and the nuclear scattering cross-sections for the irradiated condition deviate from the unirradiated reference curves (Fig. 1), implies a radially graded structure of the irradiation-induced scatterers. In the case of Fe–3wt%Ni the vacancies are deduced to be more concentrated in the core and the Ni atoms near the surface. The peak radius of the cluster size distribution is marginally larger for Fe–3wt%Ni than for pure Fe (Table 1).

The irradiation-induced hardness increase observed for Fe–3wt%Ni confirms the interpretation of the scatterers detected by SANS to be induced by irradiation. The hardness increase observed for Fe and Fe–3wt%Ni relative to the respective unirradiated conditions is similar (Table 1). This means that Ni without simultaneous addition of Cu does not cause a larger irradiation-induced hardness increase than for pure Fe. If we take into account the vacancy–Ni ratio of 0.4–0.5 derived for the average scatterer in Fe–3wt%Ni, the vacancy fractions in Fe and Fe–3wt%Ni estimated from the total volume fractions of scatterers according to Table 1 are concluded to be similar. This finding is consistent with the similar values of the measured hardness increase. So far, no effort was undertaken to separate the hardness contributions caused by loops and vacancy-solute clusters.

4. Conclusions

Measured SANS cross-sections indicate the presence of vacancy clusters or depleted zones in neutron-irradiated pure Fe. Dislocation loops detected by TEM do not cause significant scattering. A vacancy–Ni ratio of the irradiation-induced features in Fe–3wt%Ni of 0.4–0.5 can be deduced from the present observations, i.e. 2–2.5 Ni atoms combine with one vacancy on average. This finding is consistent with the measured hardness increase. The A-ratio is insensitive to the Fe fraction of the scatterers. The issue of Fe fraction can be tackled by means of atom probe investigations.

Acknowledgements

The specimens investigated were provided by Dr J. Kočík (NRI Řež). The work was supported by the European Commission in the framework of the integrated project PERFECT.

References

[1] F. Maury, A. Lucasson, P. Lucasson, P. Moser, F. Faudot, J. Phys.: Condens. Matter 2 (1990) 9291.
[2] M.K. Miller, M.A. Sokolov, R.K. Nanstad, K.F. Russell, J. Nucl. Mater. 351 (2006) 187.
[3] G.R. Odette, B.D. Wirth, D.J. Bacon, N.M. Ghoniem, MRS Bull. (March) (2001) 176–181.
[4] R. Kampmann, R. Wagner, Physica B 241–243 (1998) 36.
[5] P. Biemann, M. Haese-Seiller, P. Staron, Physica B 276–278 (2000) 156.
[6] A. Seeger, M. Rühle, Ann. Phys. 11 (1963) 216.
[7] O. Glatter, J. Appl. Cryst. 13 (1980) 7.
[8] G. Solt, F. Frisius, W.B. Waeber, P. Tipping, in: A.S. Kumar, D.S. Gelles, R.K. Nanstadt, E.A. Little (Eds.), Effects of Radiation on Materials: 16th International Symposium, ASTM STP, 1175, American Society for Testing and Materials, Philadelphia, 1993, p. 444.
[9] A. Hempel, M. Saneyasu, Z. Tang, M. Hasegawa, G. Brauer, F. Plazaola, S. Yamaguchi, F. Kano, A. Kawai, in: M.L. Hamilton, A.S. Kumar, S.T. Rosinski, M.L. Grossbeck (Eds.), Effects of Radiation on Materials: 19th International Symposium, ASTM STP, 1366, American Society for Testing and Materials, West Conshohocken, 2000, p. 560.